Available online at www.sciencedirect.com

SciVerse ScienceDirect

Advances in Space Research 51 (2013) 377–387

ADVANCES IN SPACE RESEARCH (a COSPAR publication)

www.elsevier.com/locate/asr

The nighttime anomalies using Global IGS VTEC Maps

M.P. Natali *, A. Meza

Facultad de Ciencias Astronómicas y Geofísicas, Universidad Nacional de La Plata, Paseo del Bosque s/n, (1900), La Plata, Argentina
Consejo Nacional de Investigaciones Científicas y Técnicas (CONICET), Av. Rivadavia 1917, Buenos Aires, Argentina

Received 10 April 2012; received in revised form 19 September 2012; accepted 21 September 2012
Available online 29 September 2012

Abstract

In this paper we show the VTEC variations at night, considering their geomagnetic, seasonal and solar activity dependences. The variations are analyzed in two time periods 10 p.m. (pre-midnight) and 2 a.m. (post-midnight); and for two different solar conditions; one during high solar activity (2000) and the other during low solar activity (2008). Spatial and temporal ionosphere variability is investigated from Global IGS VTEC maps applying Principal Component Analysis (PCA).

The IGS VTEC maps are reorganized and from each daily global dataset, two maps were constructed one at 10 p.m. and the other at 2 a.m. From these two series of VTEC maps covering periods low and high solar activity for each local time we found that: (1) The pre-midnight (10 p.m.) VTEC variability presents a strong semiannual anomaly at equatorial and low geomagnetic latitudes during high solar activity and in low solar activity an annual variation with maximum in summer at low-mid geomagnetic latitude. (2) The post-midnight (2 a.m) VTEC variability shows an annual variation at low and high solar activity, except in the equatorial region for high solar activity where a semiannual variation is recorded (the amplitude is twice lower than the amplitude at pre-midnight). The winter anomaly is present in the northern hemisphere in the American longitude sector and in the north-east of Africa; and a very small region in the south-west of Oceania.

Keywords: Principal Component Analysis; Global IGS VTEC maps; Anomalies; Night winter anomaly

1. Introduction

The F2 layer is anomalous rather than being simply described by the solar zenith angle as Chapman theory (1931) predicts. The mid-latitude F2 region density remains at a substantially high level during the night. A number of physical processes might be responsible for the night-time electron concentration enhancements as suggested by several authors: (1) plasma fluxes from the plasmasphere (Hanson and Ortenburger, 1961; Evans, 1965, 1975; Titheridge, 1968; Jain and Williams, 1984; Förster and Jakowski, 1988; Jakowski et al. 1991; Jakowski and Förster, 1995; Mikhailov and Förster, 1999); (2) raising of the F2-layer to higher altitudes, where the recombination rate is smaller, by electric fields and the thermospheric winds (Young et al., 1970; Standley and Williams, 1984; Hedin et al., 1991; Mikhailov et al., 2000); (3) plasma transfer from conjugate points (Balan et al., 1994) and (4) nighttime ionization at the top of the ionosphere at high latitudes (Titheridge, 1968; Leitinger et al., 1982).

The Night Winter Anomaly (NWA) is characterized by a higher nighttime F2-layer ionization level during winter months than during summer. Jakowski et al. (1981) was the first who described the NWA of the ionosphere using radio beacon measurements and vertical soundings observations at the American sector during low solar activity. In this attempt Jakowski and co-workers assumed that the considerable asymmetry in geomagnetic-geographic relationships at the American longitude sector provide good conditions for an effective interhemispheric plasma

* Corresponding author at: Facultad de Ciencias Astronómicas y Geofísicas, Universidad Nacional de La Plata, Paseo del Bosque s/n, (1900), La Plata, Argentina. Tel.: +54 221 423 6593; fax: +54 221 423 6591.

E-mail address: paula@fcaglp.unlp.edu.ar (M.P. Natali).

0273-1177/$36.00 © 2012 COSPAR. Published by Elsevier Ltd. All rights reserved.
http://dx.doi.org/10.1016/j.asr.2012.09.031

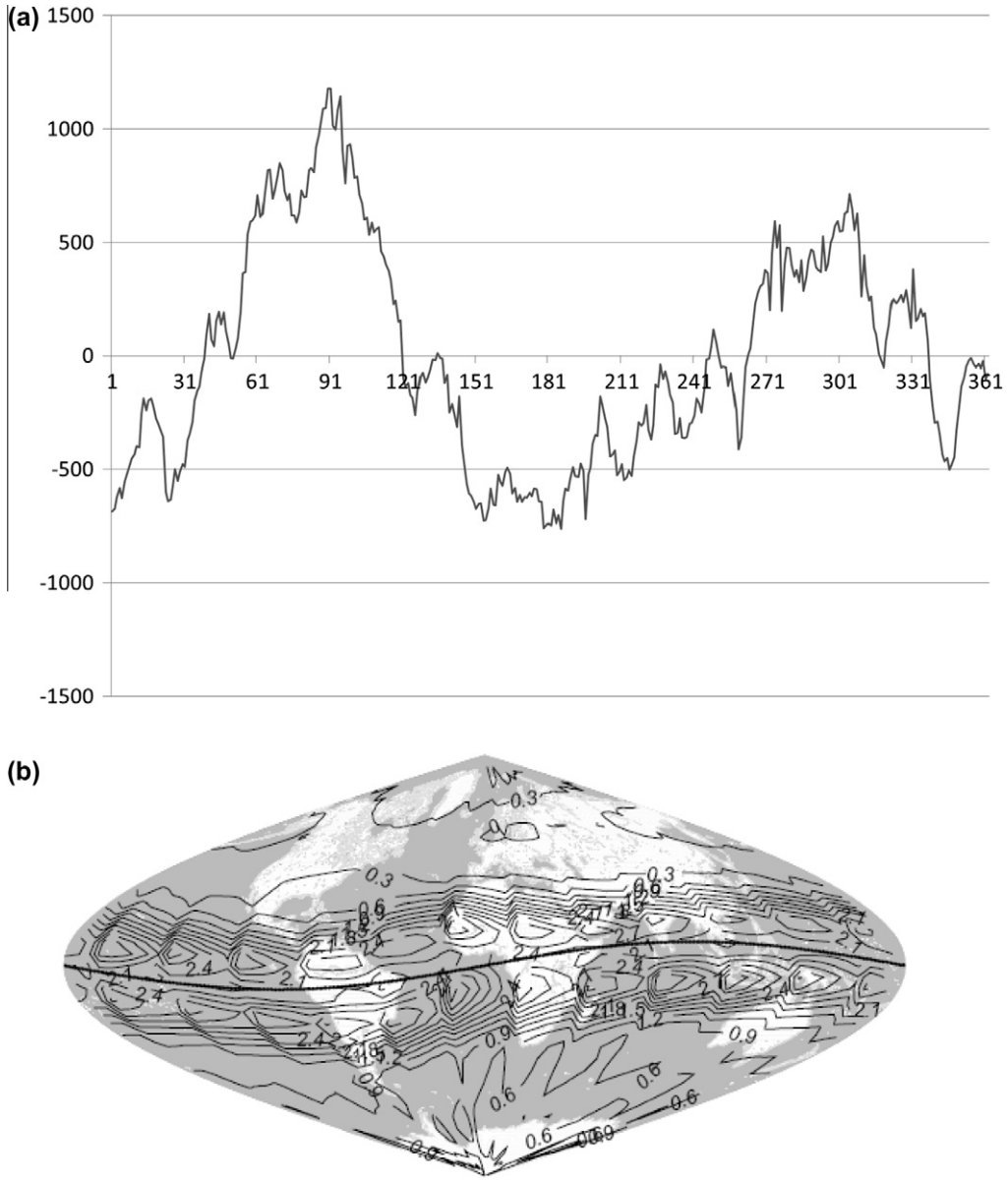

Fig. 1. (a) Time variation in the first mode for 10 p.m. local time during high solar activity. The x-axis is the day of year (DOY) and the y-axis is the amplitude multiply by a factor of 10^{-2}; (b) Spatial variation in the first mode for 10 p.m. local time.

transport from the southern (summer) hemisphere to the northern (winter) hemisphere. Due to this asymmetry the NWA is not observed at the southern hemisphere winter June/July. Förster and Jakowski (1988) observed NWA during solar minimum conditions at the American sector by means of ionospheric electron content and vertical sounding measurements in Havana (Cuba). They proposed an effective interhemispheric transport of plasma to explain enhanced northern nighttime ionization during winter solstice. Li and Yu (2002) found a noticeable annual variation in f0F2 at 2:00 LT in both hemisphere at mid-high latitudes and they did not find winter anomaly during high solar activity. They also found a semiannual variation with regional characteristics being slightly higher in South American regions.

Farelo et al. (2002) carried out a detailed study of the morphology of NmF2 nighttime enhancements over 53 ionosonde stations worldwide for different seasons and different levels of solar activity. They found that there are two distinct (pre- and post-midnight) NmF2 peaks, which can occur for any season and solar activity level. In this work was considered occurrence probability, time of occurrence and amplitude, together with their geographic, seasonal and solar activity dependence. Different mechanisms have been proposed to explain the observed variations and also different conclusions are found on seasonal and solar cycle variations of the peaks. Many authors discussed this topic considering one or two peaks of electron concentration at night but in different ways. (Young et al., 1970; Titheridge, 1973; Tyagi, 1974; Balan and Rao, 1987; Joshi and Iyer,

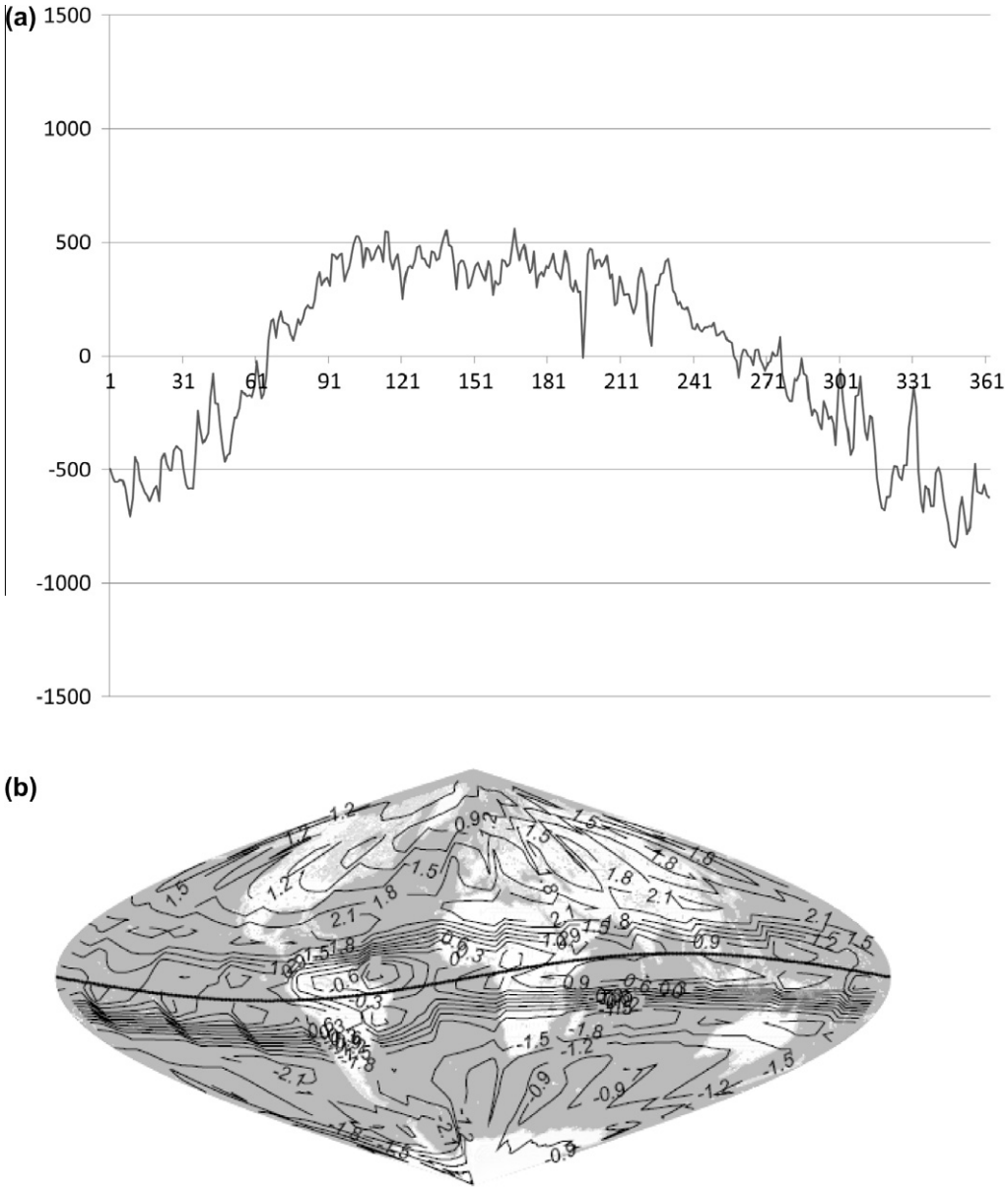

Fig. 2. (a) Time variation in the second mode for 10 p.m. local time during high solar activity. The x-axis is the day of year (DOY) and the y-axis is the amplitude multiply by a factor of 10^{-2}; (b) Spatial variation in the second mode for 10 p.m. local time.

1990) only considered the peak with higher amplitude. Many authors treated these peaks separately in their statistical analysis, but they only considered one of the peaks for each night (Jakowski et al., 1991] [Jakowski and Förster, 1995).

On May 1998 IGS created the Ionosphere Working Group (Feltens and Schaer, 1998). Among the scientific groups and institutes that are presently dedicated to ionospheric studies using GPS observations, three of them can be distinguished as the most important: the Center for Orbit Determination in Europe (CODE), that belongs to the Astronomical Institute of the University of Bern, Switzerland (http://www.aiub.unibe.ch/igs.html); the NASA Jet Propulsion Laboratory (JPL) (http://iono.jpl.nasa.gov/), Pasadena, USA; and the Astronomy and GEomatics group (gAGE) (http://gage1.upc.es/), Barcelona, Spain. The Global Ionospheric Maps (GIMs) computed by each group is made available for the users as a file in the IONosphere map EXchange (IONEX) format (Schaer et al. 1998). The file contains all the information relative to the computation process and the VTEC information are presented in the form of a grid of 2.5° in latitude and 5° in longitude.

Many researches using GPS observations have focused on the study of local and regional characteristics of ionospheric anomalies (Huang and Cheng, 1996; Unnikrishnan et al., 2002; Wu et al., 2004; Meza and Natali, 2008). Mendillo et al. (2005) have found the annual anomaly in TEC to be a global characteristic by using GIMs data, and their analysis was extended by Zhao et al. (2007), exploring the global feature of the other anomalies (winter and semiannual anomalies).

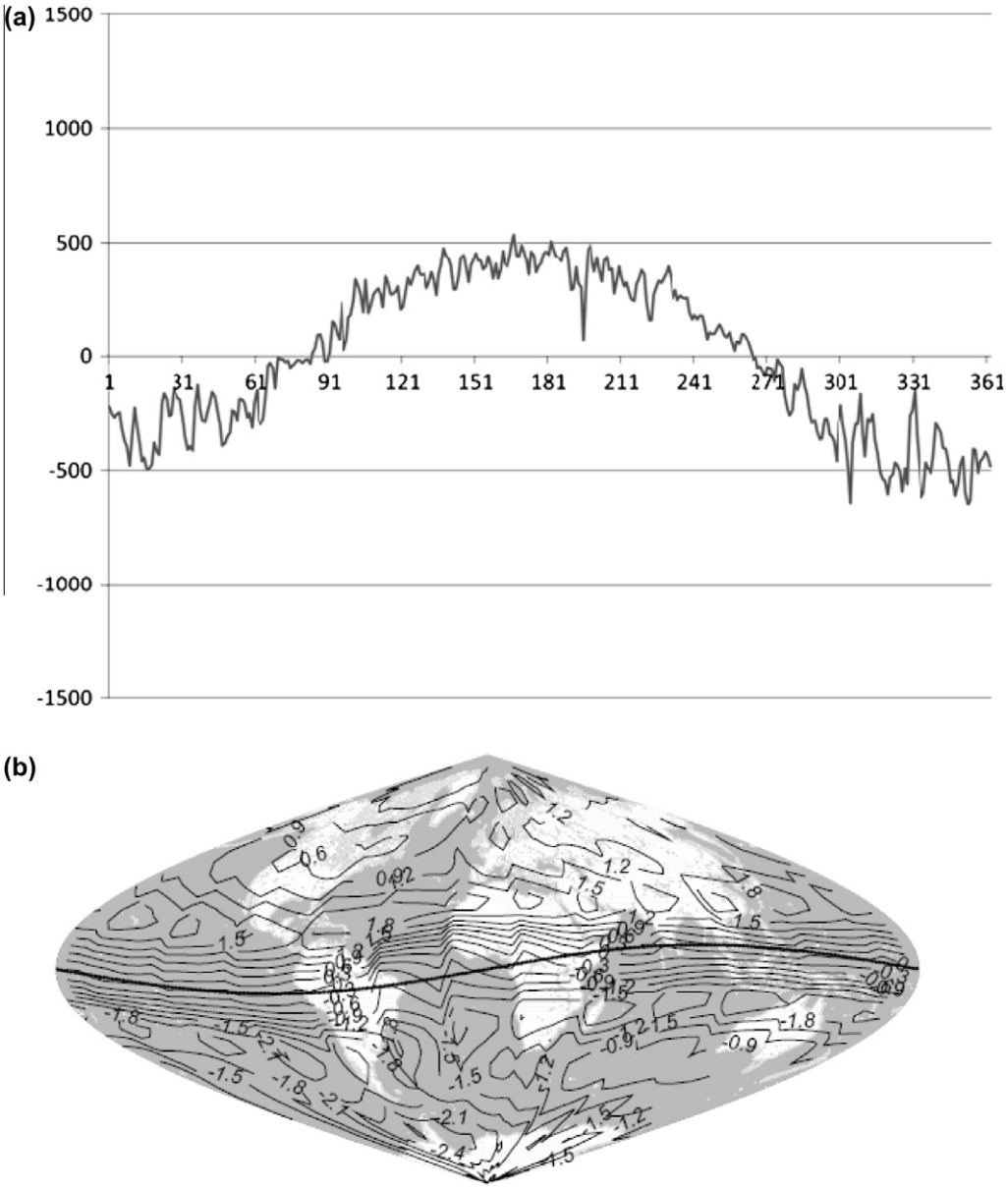

Fig. 3. (a) Time variation in the first mode for 2 a.m. local time during high solar activity. The x-axis is the day of year (DOY) and the y-axis is the amplitude multiply by a factor of 10^{-2}; (b) Spatial variation in the first mode for 2 a.m. local time.

In Natali and Meza (2010) annual, semiannual and seasonal variations of the Vertical Total Electron Content (VTEC) have been investigated during high solar activity in 2000 using Principal Component Analysis (PCA). The variations at night are smaller than those obtained at noon. In general, the semiannual behavior shows March–April equinox at least 40% higher than September one. In Meza et al. (2012) VTEC anomalies were analyzed with PCA and Wavelet Transform (WT) techniques for a complete solar cycle at 12 p.m. and 10 p.m. We found that the semiannual anomaly could be globally detected at noon during the complete solar cycle while at night the effect could only be found at high solar activity. The winter anomaly was present at night during the minima of the solar cycle. These encourage us to use the same technique to study the same anomaly at night.

In this paper we show the night variations considering their geomagnetic, seasonal and solar activity dependences. The variations will be analyzed in two time periods 10 p.m.(pre-midnight) and 2 a.m. (post-midnight); and for two different solar conditions; one during high solar activity (2000) and the other during low solar activity (2008). Spatial and temporal ionosphere variability is investigated from Global IGS VTEC maps (GIMs) applying Principal Component Analysis (PCA).

2. Methodology

The IONEX format allows the storage of snapshots of the electron density (including associated rms information) referring to particular epochs and to a 2 or 3 dimensional, Earth-fixed grid. IONEX data supply a good estimation of

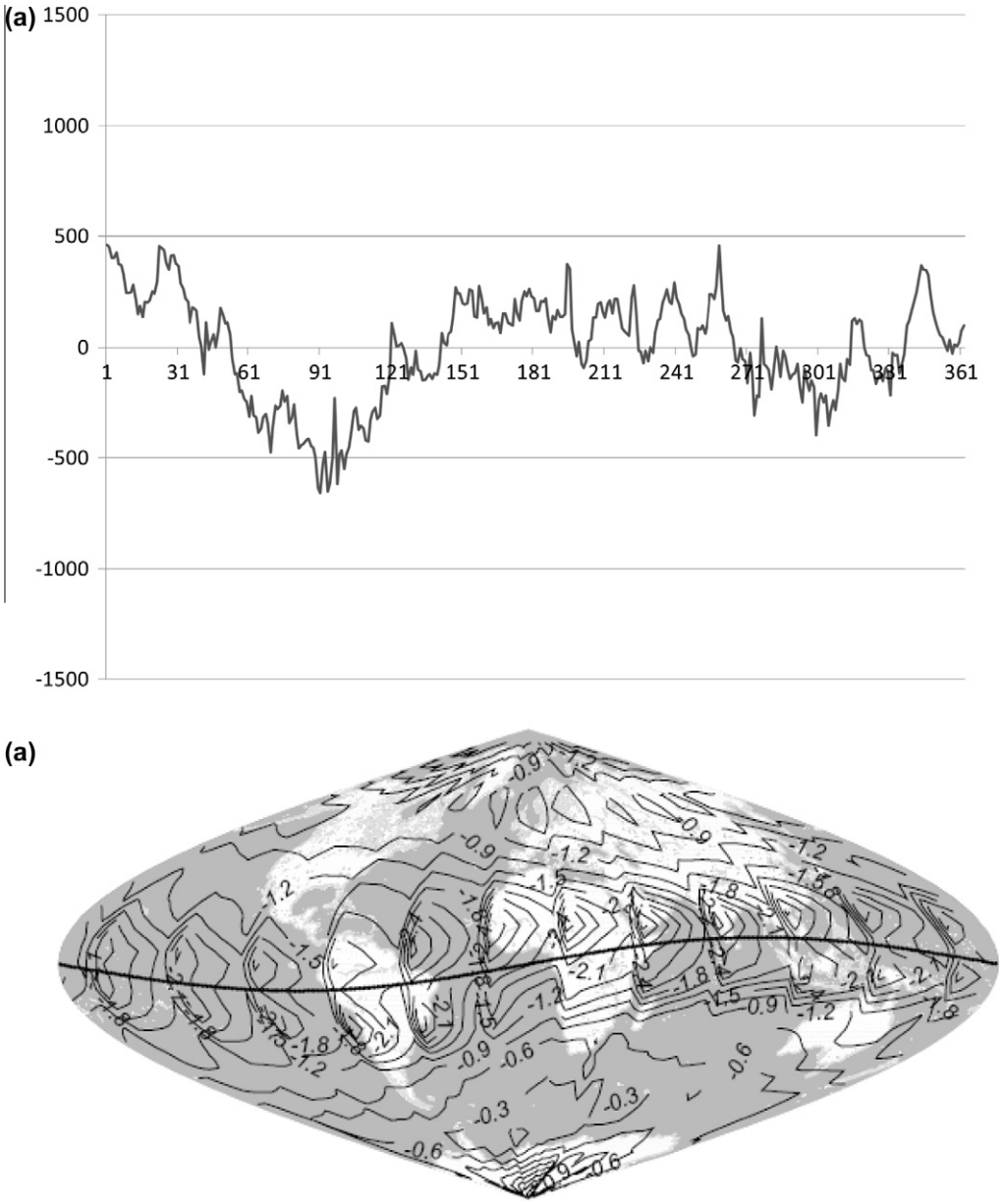

Fig. 4. (a) Time variation in the second mode for 2 a.m. local time during high solar activity. The x-axis is the day of year (DOY) and the y-axis is the amplitude multiply by a factor of 10^{-2}; (b) Spatial variation in the second mode for 2 a.m. local time.

the worldwide VTEC. These data provide VTEC values around the world at intervals of 2.5° in latitude and 5° in longitude.

Global IGS VTEC maps during high solar activity (2000) and low solar activity (2008) are used in this work. This VTEC maps show a global snapshot of the ionosphere every two hours. Therefore, the main geographical VTEC variation that can be seen on them is the ionization due to solar radiation. Since we are not interested in analyzing that effect but the ionospheric response to similar solar radiation conditions on different locations, we reorganized the VTEC data as follows: from each daily global datasets, composed by twelve hourly VTEC maps, we selected the map center at local time 10 p.m. (pre-midnight) and 2 a.m. (post-midnight). In this way we could analysis in two significantly different solar activity conditions. The temporal series were constructed in the following way: assuming that the ionosphere doesn't change in a two hour window, we took 30 degree slices from all VTEC maps for each day, centered on the same local time. These slices were then merged into a new VTEC map according to their central longitude. This procedure resulted in two new VTEC maps per day, corresponding to the two different local times selected.

2.1. PCA application

PCA is used to identify spatial structures that have dominant contribution to the total variability together with their time evolution.

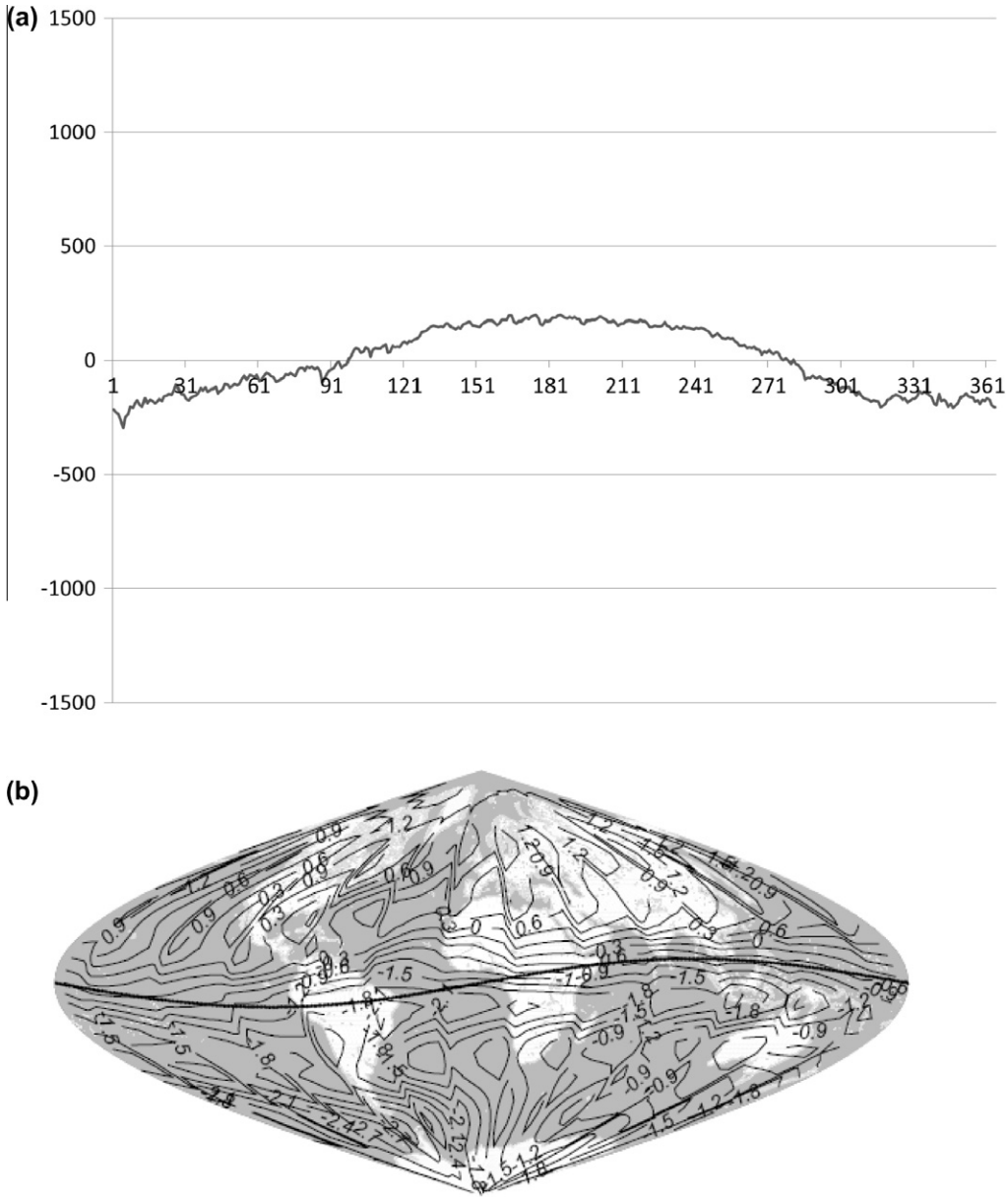

Fig. 5. (a) Time variation in the first mode for 10 p.m. local time during low solar activity. The x-axis is the day of year (DOY) and the y-axis is the amplitude multiply by a factor of 10^{-2}; (b) Spatial variation in the first mode for 2 a.m. local time.

PCA is well suited for the analysis of multivariate time series. One main reason for that is that the technique can be used to identify spatial structures that have dominant contribution to the total variability together with their time evolution without the need to propose any particular a priori functional model.

PCA is used to express a correlated data set on a new orthonormal base of minimum dimension. The shape of the base functions is determined from the data set itself. This method is of special interest when the phenomena under study are not necessarily a superposition of well-known simple components that would point other techniques (e.g., Fourier analysis) as more adequate.

The first step in PCA is to center the time series on their time averages. Using this new time series we construct the symmetric scatter matrix.

Let z(t, x) be VTEC measures, at point x (latitude and longitude) in the atmosphere at time t. Let these measurements be taken over the set of locations $x = 1, \ldots, p$ at times $t = 1, \ldots, n$. The first step in PCA is to center the time series on their time averages. This is,

$$\mathbf{z}'(t,x) = \mathbf{z}(t,x) - \bar{\mathbf{z}}(t,x) \tag{2.1}$$

$$\text{with,} \quad \bar{\mathbf{z}}(t,x) = \frac{\sum_{t=1}^{n} \mathbf{z}(t,x)}{n} \tag{2.2}$$

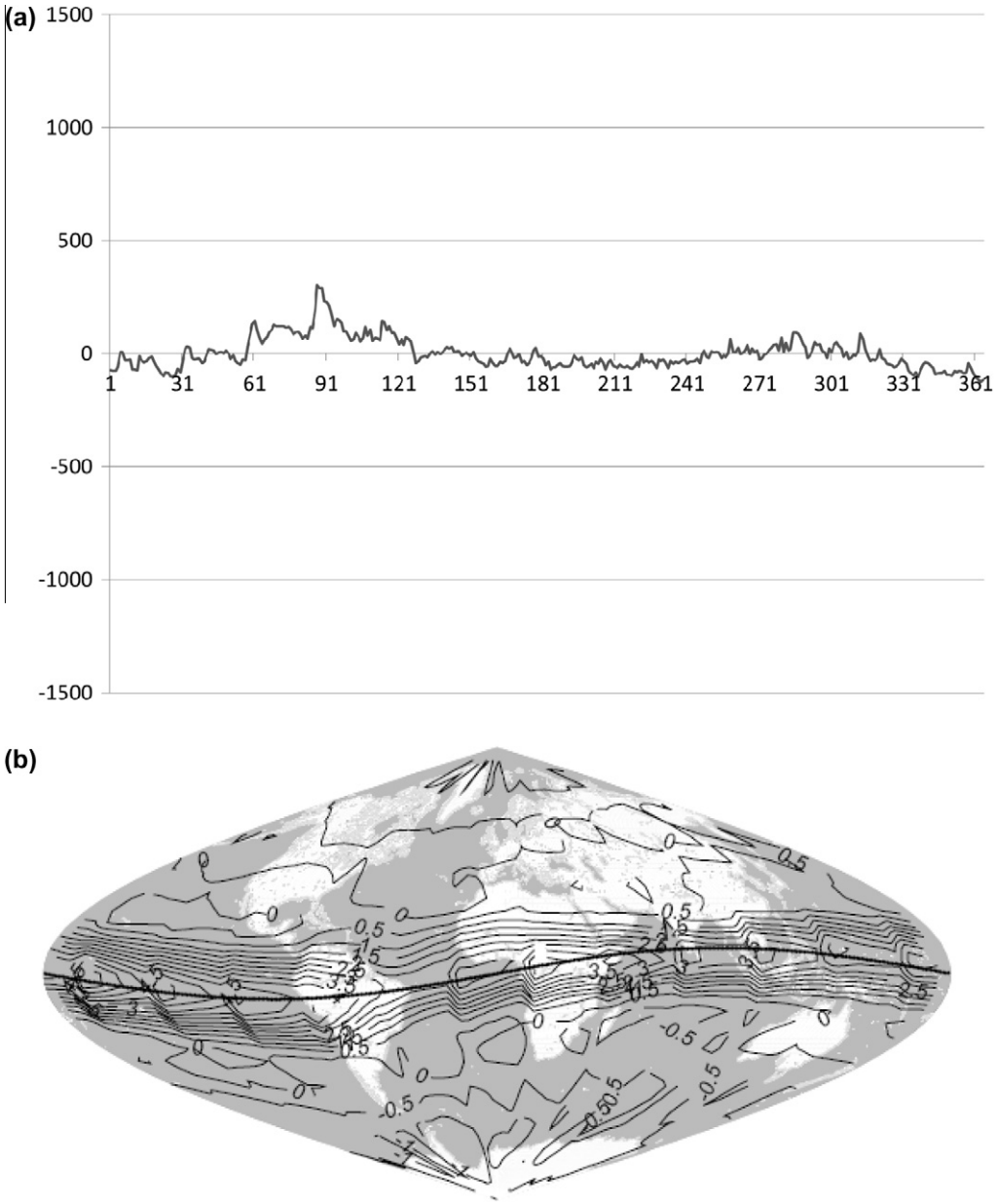

Fig. 6. (a) Time variation in the second mode for 10 p.m. local time during high solar activity. The x-axis is the day of year (DOY) and the y-axis is the amplitude multiply by a factor of 10^{-2}; (b) Spatial variation in the second mode for 10 p.m. local time.

These collections can be thought as $p \times 1$ (i.e., column) vectors $\mathbf{z}'(t) = \{\mathbf{z}'(t,1),\ldots,\mathbf{z}'(t,p)\}$ forming a swarm of points about the origin of a p-dimensional Euclidean space (Ep). Now it is possible to construct the symmetric scatter matrix, $\mathbf{S}$, in the p-dimensional Euclidian space, Ep.

$$\mathbf{S} = \sum_{t=1}^{n} \mathbf{z}'(t)\mathbf{z}'^{T}(t) \tag{2.3}$$

This matrix has a set of p orthonormal eigenvectors $\mathbf{e}_j$. From these $\mathbf{e}_j$ we can construct the principal components (or amplitudes) of the data set, $\mathbf{a}_j(t)$:

$$\mathbf{a}_j(t) = \sum_{x=1}^{p} \mathbf{z}'(t,x)\mathbf{e}_j(x) = \mathbf{z}'(t)^{\mathrm{T}}\mathbf{e}_j \qquad \text{(Analysis of } \mathbf{z}') \tag{2.4}$$

$$t = 1,\ldots,n;\ j = 1,\ldots,p$$

These $\mathbf{a}_j(t)$, can be thought of as a family of time series $\{\mathbf{a}_j(t)\colon t = 1,\ldots,n\}$. The most important property of these time series is that they are mutually uncorrelated, carrying information about the variance of the data set along the directions $\mathbf{e}_j$.

Finally, and most importantly, the original centered data set can be exactly represented in the form

$$\mathbf{z}'^{\mathrm{T}}(t,x) = \sum_{j=1}^{p} a_j(t)\mathbf{e}_j^{\mathrm{T}}(x) \qquad \text{(Synthesis of } \mathbf{z}') \tag{2.5}$$

$$t = 1,\ldots,n;\ x = 1,\ldots,p.$$

By eigenvalue decomposition of the covariance matrix of VTEC variations the PCA technique identifies those spatial

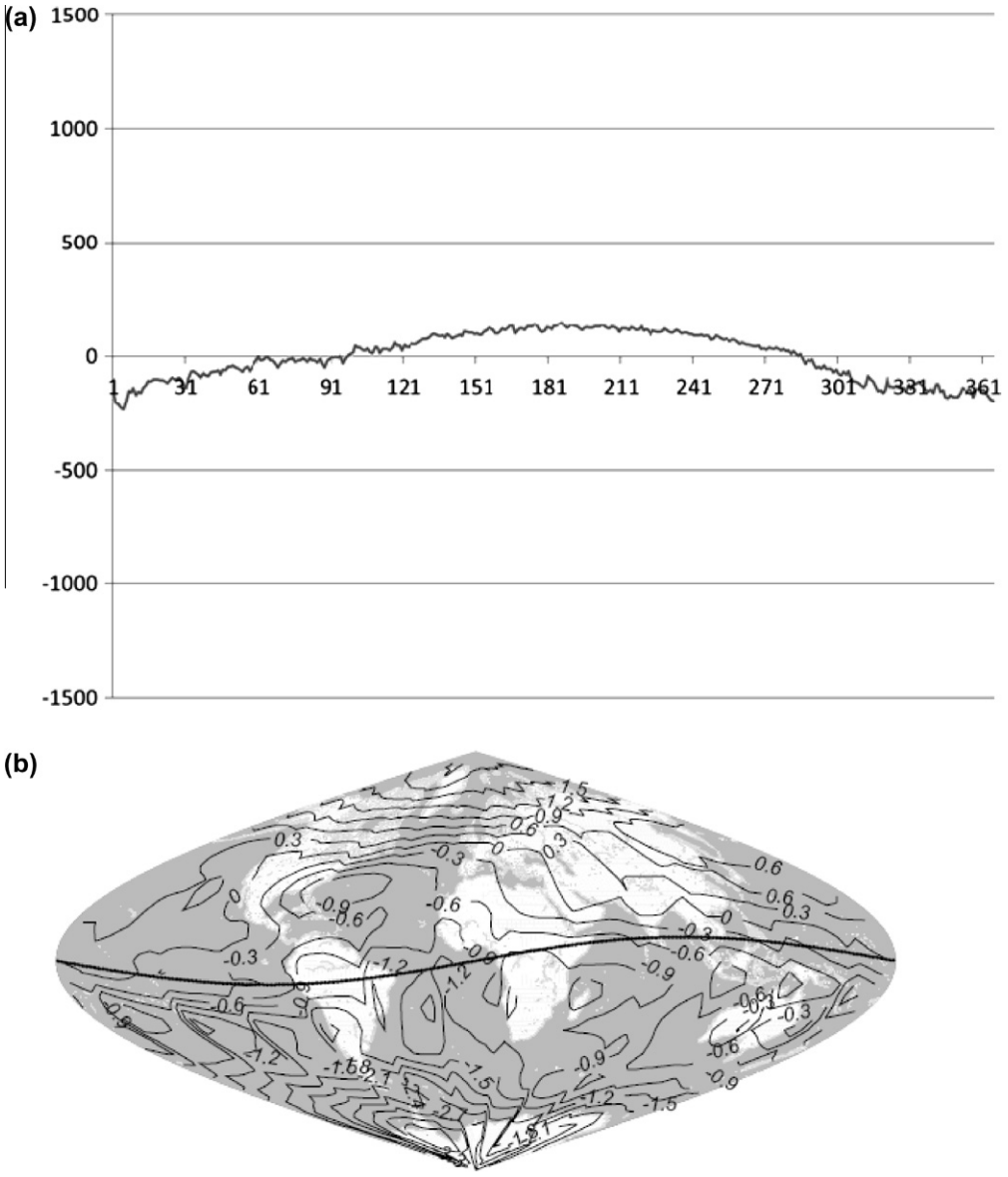

Fig. 7. (a) Time variation in the first mode for 2 a.m. local time during low solar activity. The *x*-axis is the day of year (DOY) and the *y*-axis is the amplitude multiply by a factor of 10^{-2}; (b) Spatial variation in the first mode for 2 a.m. local time.

structures of the ionospheric variability that have dominant contribution to the total variance. The spatial structure of the ionospheric variability is represented by the eigenvector ($\mathbf{e}_j$) and its temporal evolution is described by a series of coefficients ($\mathbf{a}_j$), called principal components. Eigenvector and principal components together are called mode. Modes are ordered according to decreasing eigenvalues, such the first mode represents the largest part of the variance, the next mode the second largest part, etc. This method is a powerful tool because the principal components have the information of the original data, which means, the orthonormal functions are directly determined by the data itself. For further details of the foundations and methodology applied in this work see (Preisendorfer, 1988; Meza and Natali, 2008).

3. Results

The VTEC behavior is studied in two time periods 10 p.m. (pre-midnight) and 2 a.m. (post-midnight); and for two different solar conditions; one during high solar activity (2000) and the other during low solar activity (2008). These epochs correspond to two different times of series once the VTEC grids are built for every day and every year. PCA analysis was applied to each time series in order to estimate the amplitudes ($\mathbf{a}_j$) and eigenvectors ($\mathbf{e}_j$) associated to each data set (Eqs. (2.4) and (2.5)).

For this dataset, we found that the first two PCA modes contain approximately 80% of the total VTEC variability. Modes 1 and 2 can be written as the products ($\mathbf{a_1} \cdot \mathbf{e_1}$) and ($\mathbf{a_2} \cdot \mathbf{e_2}$) respectively, where $\mathbf{e}_j$ contains the spatial

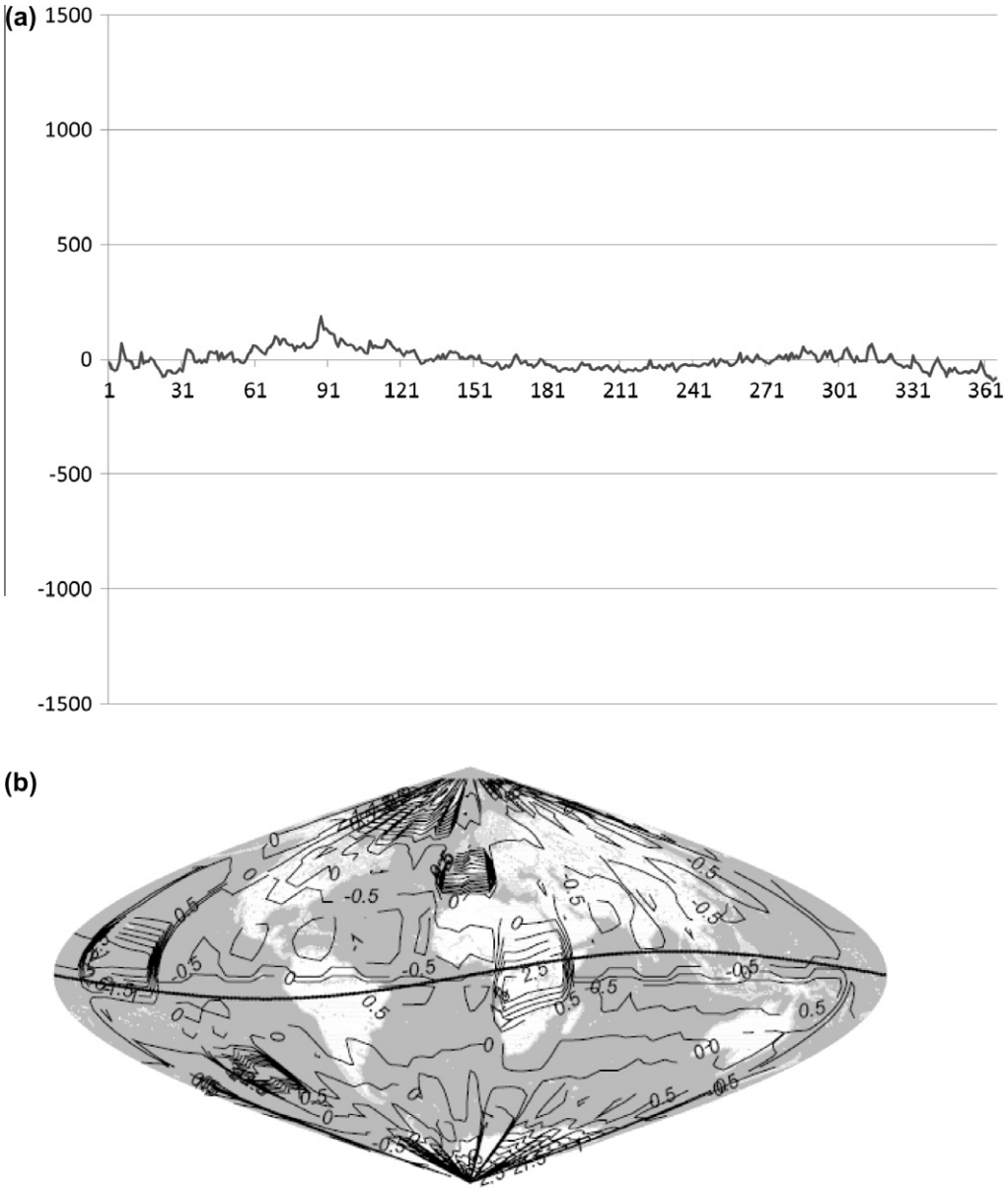

Fig. 8. (a) Time variation in the second mode for 2 a.m. local time during low solar activity. The x-axis is the day of year (DOY) and the y-axis is the amplitude multiply by a factor of 10^{-2}; (b) Spatial variation in the second mode for 2 a.m. local time.

variation and the $\mathbf{a}_j$ contains the temporal variation of the data set. $\mathbf{e}_j$ and $\mathbf{a}_j$ are adimensional, the units of the product of $\mathbf{e}_j$ and $\mathbf{a}_j$ are TECU (1 TECU $= 10^{16}$ electron/m^2). Thus, there are 8 PCA amplitudes data time series: mode 1 and mode 2 at 10 p.m. (pre-midnight) local time and mode 1 and mode 2 at 2 a.m. local time (post-midnight) for two solar conditions; high solar activity (2000) and low solar activity (2008).

The results of the application of the PCA technique on VTEC data are showed in Figs. 1–8. Because we analyzed mode 1 and mode 2 at local pre-midnight and post-midnight and for two different solar activities there are eight figures. Each figure is a composite panel of two plots formed by: the PCA eigenvector variability ($\mathbf{e}_j$) and the PCA amplitude variability ($\mathbf{a}_j$).

3.1. High solar Activity: Pre-midnight (10 p.m.) (Figs. 1 and 2)

The first mode shows strong semiannual component, the contribution to the variance is 50%. From Fig. 1 the semiannual anomaly is present at low and equatorial geomagnetic latitudes. The maximum VTEC amplitudes variations reached values between 12 and 24 TECU ($\mathbf{a}_1 \cdot \mathbf{e}_1$) in these regions.

The second mode (32% of the variance contribution) shows variation with maximum values in summer solstice and minimum in winter solstice, mainly at mid-high geomagnetic latitudes (Fig. 2). The maximum VTEC amplitudes variations reached values between 6 to 10 TECU ($\mathbf{a}_2 \cdot \mathbf{e}_2$) in these regions.

3.2. High solar Activity: Post-midnight (2 a.m.) (Figs. 3 and 4)

The first mode shows an annual component with maximum values in summer solstice and minimum in winter solstice. The contribution to the variance is 47%. From Fig. 3 the annual component is present at mid-low geomagnetic latitudes and at high geomagnetic latitudes in South America and west Asia sectors. The maximum VTEC amplitudes variations at mid-low geomagnetic latitudes doṅt exceed 9 TECU ($\mathbf{a}_1 \cdot \mathbf{e}_1$) and for high geomagnetic latitudes in South America and west Asia sectors reached values around 11 TECU.

The second mode (24% of the variance contribution) shows a semiannual variation with maximum values at low equatorial geomagnetic latitudes (Fig. 4). In this region the maximum VTEC amplitudes variations reached values between 6 to 9 TECU ($\mathbf{a}_2 \cdot \mathbf{e}_2$).

3.3. Low solar Activity: Pre-midnight (10 p.m.) (Figs. 5 and 6)

The first mode shows an annual component, the contribution to the variance is 64%. From Fig. 5 the annual component is present mainly at mid-low geomagnetic latitudes reaching maximum VTEC amplitudes variations up to 4 TECU ($\mathbf{a}_1 \cdot \mathbf{e}_1$)and at high geomagnetic latitudes in South America, in the South Pacific Ocean and in the north-west of Asia, in this region the VTEC variations goes up to 7 TECU. At high latitudes the amplitudes are larger in far polar geomagnetic regions. The winter anomaly is present in a small region in the north of South America, showing VTEC variations up to 3 to 4 TECU.

The second mode (15% of the variance contribution) shows a semiannual variation in equatorial geomagnetic latitudes (Fig. 6). The maximum VTEC amplitude variations reached values up to 7 TECU ($\mathbf{a}_2 \cdot \mathbf{e}_2$).

3.4. Low solar Activity: Post-midnight (2 a.m.) (Figs. 7 and 8)

The first mode shows an annual component, the contribution to the variance is 66%. From Fig. 7 the annual component is present in the southern hemisphere and at high geomagnetic latitudes in the northern hemisphere reaching values up to 3 TECU ($\mathbf{a}_1 \cdot \mathbf{e}_1$). The winter anomaly is recorded at the northern hemisphere in the American longitude sector; in the north-east of Africa and a very small region in the south-west of Oceania, in both regions the maximum VTEC amplitude variations reach values around 1 TECU ($\mathbf{a}_2 \cdot \mathbf{e}_2$).

The second mode (11% of the variance contribution) shows a weak semiannual variation (Fig. 8).

4. Summary and discussion

The IGS ionospheric product, called IONEX file, provides very useful information to investigate the night time anomaly. The analysis at night time is separated in two intervals: pre- and post-midnight. The PCA technique is a numerical tool used to separates the main orthogonal component (called modes) of the VTEC scattering.

During high solar activity the semiannual anomaly is mainly recorded at equatorial and low geomagnetic latitudes, prevailing the anomalous behavior during noon time (Natali and Meza, 2011). The semiannual anomaly is also present at post-midnight at the same region and its amplitude is two times lower than pre-midnight. This VTEC variation at low and equatorial latitudes could owe to the effect combined of the maximum [O/N_2] concentration and minimum values of the prevailing wind in equinox. Other contribution could be the semiannual variation of the equatorial electrical jet, solar wind and geomagnetic activity. The annual variability is recorded at mid geomagnetic latitude and at high geomagnetic latitudes in both hemispheres as was found by Li and Yu (2002) especially in far geomagnetic Polar Regions, reaching maximum values in summer. Our results confirm that there are strong increases of the night time ionization in summer.

During low solar activity the annual component is present at mid-low geomagnetic latitudes and at high geomagnetic latitudes in South America, in the South Pacific Ocean and in the north-west of Asia at pre-midnight. It is possible to see the winter anomaly in a small region in the northern part of South America. At post-midnight the annual component is present in the southern hemisphere and at high geomagnetic latitudes in the northern hemisphere. The winter anomaly is recorded at the northern hemisphere in the American longitude sector and in the north-east of Africa; and a very small region in the south-west of Oceania as was found by Jakowski and Förster (1995). These authors showed that numerical modeling supports interhemispheric coupling via plasma fluxes along magnetic flux tubes as a possible explanation for the NWA.

References

Balan, N., Rao, P.B. Latitudinal variations of night-time enhancements in total electron content, J. Geophys. Res. 92, 3436–3440, 1987.

Balan, N., Bailey, G.J., Balachandran Nair, T., Titheridge, J.E. Nighttime enhancements in ionopheric electron content in the northern and southern hemispheres. J. Atmos. Terr. Phys. 56, 67–79, 1994.

Chapman, S. The absorption and dissociatival or ionizing effect of monochromatic radiation in atmosphere on a rotating earth. Proc. Phys. Soc. 43, 483–501, 1931.

Evans, J.V. Cause of midlatitude winter increase in f0F2. J. Geophys. Res. 70, 4331–4345, 1965.

Evans, J.V. A study of F2 region night-time vertical ionization fluxes at Millstone Hill. Planet. Space Sci. 18, 1225–1253, 1975.

Farelo, A.F., Herraiz, M., Mikhailov, V. Global morphology of night-time NmF2 enhancements, Ann. Geophys. 20, 1795–1806, 2002.

Feltens, J., Schaer. S. IGS Products for the Ionosphere, in: Dow, J.M., Kouba, J. Springer, T. (Eds.), Proceedings of the IGS Analysis Center Workshop, Darmstadt, pp. 225–232, February 9–11, 1998.

Förster, M., Jakowski, N. The nighttime winter anomaly (NWA) effect in the American sector as a consequence of interhemispheric ionospheric coupling. PAGEOPH 127, 447–471, 1988.

Hanson, W.B., Ortenburger, I.B. The coupling between the protonosphere and the normal F-region. J. Geophys. Res. 66, 1425–1435, 1961.

Hedin, A.E., Biondi, M.A., Burnside, R.G., Hernandez, G., Johnson, R.M., Killen, T.L., Mazaudier, C., Meriwether, J.W., Salah, J.E., Sica, R.J., Smith, R.W., Spencer, N.W., Wickar, V.B., Virdi, T.S. Revised global model of thermosphere winds using satellite and ground-based observations. J. Geophys. Res. 96 (A5), 7657–7688, 1991.

Huang, Y.N., Cheng, K. Solar cycle variations of the equatorial ionospheric anomaly in total electron content in the Asian region. J. Geophys. Res. 101, 24513–24520, 1996.

Jain, A.R., Williams, P.J.S. The maintenance of nighttime ionosphere at mid-latitudes. II. The ionosphere above St. Santin. J. Atmos. Terr. Phys. 46, 83–89, 1984.

Jakowski, N., Förster, M. About the nature of the nighttime winter anomaly effect (NWA) in the F-region of the ionosphere. Planet Space Sci. 43, 603–612, 1995.

Jakowski, N., Bettac, H.D., Lazo, B., Lois, L. Seasonal variations of the columnar electron content of the ionosphere observed in Havana from July 1974 to April 1975. J. Atmos. Terr. Phys. 43, 7–11, 1981.

Jakowski, N., Jungstand, A., Lazo, A., Lois, L. Night-time enhancement of the F2-Layer ionization over Havana. Cuba. J. Atmos. Terr. Phys. 53, 1131–1138, 1991.

Joshi, H.P., Iyer, K.N. On night-time anomalous enhancement in ionopheric electron content al lower mid-latitude during solar maximum. Ann. Geophys. 8, 53–58, 1990.

Leitinger, R.G., Hartmann, G.K., Degenhart, W., Hedberg, A., Tanskanen, P. The electron content of the ionosphere and the southern boundary of diffuse aurora. J. Atmos. Terr. Phys. 44, 369–374, 1982.

Li, X., Yu, T. Annual and Semi-annual variations of the observed foF2 in a high solar activity year. Terr. Atmos. Ocean. Sci. 14 (1), 41–62, 2002.

Mendillo, M., Huang, C.-L., Pi, X.-Q., Rishbeth, H., Meier, R.R. The global asymmetry in ionospheric total content. J. Atmos. Sol. Terr. Phys. 67, 1377–1387, 2005.

Meza, A., Natali, M.P. Annual and semiannual TEC effects at low solar activity in midlatitude Atlantic region based on TOPEX. J. Geophys. Res. 113, D14115, http://dx.doi.org/10.1029/2007JD009088, 2008.

Meza, A., Natali, M.P., Fernández, L.I. Analysis of the winter and semiannual ionospheric anomalies in 1999-2009 based on GPS global International GNSS Service maps. J. Geophys. Res. 117, A01319, http://dx.doi.org/10.1029/2011JA016882, 2012.

Mikhailov, A.V., Förster, M. Some F2-layer effects during the 6–11 January 1997 CEDAR storm period as observed with the Millstone Hill incoherent scatter facility. J. Atmos. Sol. Terr. Phys. 61, 249–261, 1999.

Mikhailov, A.V., Leschinkaya, T.Yu, Förster, M. Morphology of NmF2 night-time increases in the Eurasian sector. Ann. Geophys. 18, 618–628, 2000.

Natali, M.P., Meza, A. Annual and semiannual VTEC effects at low solar activity based on GPS observations. J. Geophys. Res. 115, D18106, http://dx.doi.org/10.1029/2010JD014267, 2010.

Natali, M.P., Meza, A. Annual and semiannual variations of vertical total electron content during high solar activity based on GPS observations. Ann. Geophys. 29, 865–873, 2011.

Preisendorfer, R.W. Principal Component Analysis in Meteorology and Oceanography. Elsevier, Amsterdam, 424 p, 1988.

Schaer, S., Beutler, G., Rothacher, M. Mapping and predicting the ionosphere, in: Proceedings of the IGS AC Workshop, Darmstadt, Germany, 1998.

Standley, P.J., Williams, P.J.S. The maintenance of nighttime ionosphere at mid-latitudes. I. The ionosphere above Malvern. J. Atmos. Terr. Phys. 46, 73–81, 1984.

Titheridge, J.E. The maintenance of the nighttime ionosphere. J. Atmos. Terr. Phys. 30, 1857–1875, 1968.

Titheridge, J.E. The electron content of the southern mid-latitude ionosphere. J. Atmos. Ter. Phys. 30, 1857–1875, 1973.

Tyagi, T.R. Electron content and its variation over Lindau. J. Atmos. Terr. Phys. 36, 475–487, 1974.

Unnikrishnan, K., Nair, R.B., Venugopal, C. Harmonic analysis and an empirical model for TEC over Palehua. J. Atmos. Sol. Terr. Phys. 64, 1833–1840, 2002.

Wu, C.C., Fryb, C.D., Liu, J.Y., Lioud, K., Tseng, C.L. Annual TEC variation in the equatorial anomaly region during the solar minimum: September 1996 – August 1997. J. Atmos. Sol. Terr. Phys. 66, 199–207, 2004.

Young, D.M.L., Yuen, P.C., Roelofths, T.H. Anomalous night-time increases in total electron content. Planet Space Sci. 18, 1163–1179, 1970.

Zhao, B., Wan, W., Liu, L., Mao, T., Ren, Z., Wang, M., Christensen, A.B. Features of annual and semiannual variations derived form the global ionospheric maps of total electron content. Ann. Geophys. 25, 2513–2527, 2007.